# Interfacial Morphology Development during PS/PMMA Reactive Coupling

**Jianbin Zhang, Timothy P. Lodge,* and Christopher W. Macosko***

*Department of Chemical Engineering and Materials Science, and Department of Chemistry, University of Minnesota, Minneapolis, Minnesota 55455*

*Received March 11, 2005; Revised Manuscript Received June 3, 2005*

ABSTRACT: Amine-terminal polystyrene (PS-$NH_2$) was reacted with an anhydride-terminal poly(methyl methacrylate) (PMMA-anh-pyr) at the interface between quiescent PS and PMMA layers, annealed for various times up to 2 h at 175 °C. The concentration of the PS-$NH_2$ in the PS layer was varied from 10% to 100%. By virtue of pyrene labeling, the PMMA-anh-pyr conversion to copolymer in the early stages of the reaction could be measured with a fluorescence detector coupled to a size exclusion chromatograph. Interfacial morphology development was monitored with both atomic force microscopy (AFM), after washing off the top PS layer, and transmission electron microscopy (TEM), in cross section. It was found that the coupling reaction at the initial stage is rapid. Detectable block copolymer interfacial coverage ($\Sigma$) and interfacial roughness were obtained even after only 5 min annealing. Further annealing the samples increased $\Sigma$ significantly when the PS-$NH_2$ concentration exceeded 25%. In this case $\Sigma$ exceeded the value expected for a saturated monolayer of copolymer $\Sigma^*$, suggesting emulsification at the interface. The surface roughness determined by AFM supports this conclusion, as the RMS roughness is low when $\Sigma < \Sigma^*$ but increases dramatically when $\Sigma > \Sigma^*$. After the emulsification transition, however, the AFM roughness no longer increases because the emulsified material is washed away with the PS layer. With TEM, the emulsified region could be observed at the interface directly. Furthermore, the interfacial roughness values from AFM and TEM agree well.

## Introduction

Reactive compatibilization is used extensively in the processing of immiscible polymer blends.[1−3] When polymer chains with complementary functional groups meet at an interface during mixing, they can react to form block or graft copolymers and thereby reduce interfacial tension and suppress coalescence, resulting in a stabilized blend. Given the importance of reactive compatibilization, it is desirable to gain a fundamental understanding of the molecular factors controlling copolymer formation at the interface. During the past decade, the coupling reaction of functional polymers at flat, immiscible polymer−polymer interfaces has been widely studied using bilayer samples as a model system.[4−16] Many aspects of the reaction have been investigated, including the reaction kinetics, the interfacial morphology development, and the interfacial adhesion. Of particular interest is the evolution of the interfacial structure, as copolymer formation first reduces the interfacial tension and subsequently leads to emulsification.

Interfacial roughening during annealing of reactive layered samples was first studied independently by Lyu et al. and by Jiao et al. using AFM and TEM.[4,5] With AFM, solvent was used to remove the top layer, and the revealed surface was found to have roughened as a function of reaction time. With TEM, the cross section of the interface was examined, and an emulsified region was observed at the interface. Similar phenomena were observed by other researchers.[8,13] It is believed that the interfacial roughening or interfacial emulsification is induced by the coupling reaction of the functional polymer. However, it is an open question as to how this roughening is related to the extent of the coupling reaction. Jiao et al. observed a rather sharp increase in the root-mean-square (RMS) roughness by AFM as block copolymer concentration at the interface increases.[5] Similar behavior was also reported by Schulze in some cases, while for different molecular weights of the functional polymer or matrix polymer, a constant RMS or even decreasing roughness was observed over the entire reaction time.[17] Clearly, more work is needed to more closely relate the interfacial roughening process with the coupling reaction. So far, both TEM and AFM have been used to characterize the roughening processing at interfaces. On one hand, AFM allows a quantitative measurement of roughness over a substantial area, whereas TEM only provides a snapshot of a fractured cross section. However, AFM requires removal of one layer, and consequently it may not be possible to observe emulsification as the copolymer-rich region may be washed away as well. In this paper we attempt to correlate the results from these two techniques. Furthermore, using a fluorescently labeled reactant provides sufficient sensitivity that the extent of the coupling reaction can be measured precisely as a function of reaction time, to provide a direct correlation between interfacial structure and copolymer conversion.

This work describes the interfacial roughening process at polystyrene (PS)/poly(methyl methacrylate) (PMMA) interfaces. Amine-terminal PS (PS-$NH_2$) and pyrene-labeled, anhydride-terminal PMMA (PMMA-anh-pyr) serve as the model system. The coupling reaction was controlled by adjusting the concentration of PS-$NH_2$ in a nonreactive PS matrix of the same molecular weight, while maintaining the same pure PMMA-anh-pyr layer. Interfacial morphology development was measured by both AFM and TEM, and reaction conversion was monitored by size exclusion chromatography with fluorescence detection. With both reaction conversion and interfacial roughness known, the coupling reaction and interfacial morphology development can be directly related.

* To whom correspondence should be addressed. E-mail lodge@chem.umn.edu, macosko@umn.edu.

10.1021/ma050530l CCC: $30.25 
Published on Web 07/01/2005

**Table 1. Characteristics of Polymers Used in This Work**

| polymer | $M_n$ (kg/mol) | $M_w/M_n$ | $f$ (coupling) | $f$ ($^{19}$F NMR) |
|---|---|---|---|---|
| PS-CN | 18 | 1.20 | | |
| PS-$NH_2$ | 18 | 1.20 | 1.00 | 0.97 |
| PMMA-anh-pyr | 23 | 1.27 | 1.00 | |

## Experimental Section

**Materials.** The characteristics of the polymers used in this work are listed in Table 1. They were synthesized following Scheme 1. A nitrile-terminal PS (PS-CN), which was also used as the precursor for amine-terminal PS (PS-$NH_2$), was synthesized by atom transfer radical polymerization (ATRP). The initiator (2-bromoproponitrile) and the catalysts (including CuBr, Cu, and bipyridine) were purchased from Aldrich and used as received. Styrene was passed through a pad of basic alumina (Brockman I) and purged with argon for 30 min before use. The synthesis was performed in bulk at 110 °C for 24 h. The crude reaction mixture was then dissolved in dry tetrahydrofuran (THF) and passed through a short alumina column to remove the copper complex. The PS-CN product was precipitated in methanol and dried in a vacuum oven at 50 °C for a week. To obtain PS-$NH_2$, PS-CN was reduced with $LiAlH_4$ in THF solution at room temperature for 24 h. The reaction was then quenched by sequential addition of aqueous sodium hydroxide (15% NaOH) and water. The final product PS-$NH_2$ was purified by filtration of the solution through a pad of silica gel and precipitation into methanol. Anhydride-terminal PMMA (PMMA-anh-pyr) was also synthesized by ATRP following Malz et al.[18] The initiator used was bromo-4-methylphthalic anhydride, which was made from 4-methylphthalic anhydride supplied by Avecia and used as received. A pyrene-labeling group was randomly incorporated into the PMMA chain, with approximately one pyrene moiety per chain following Moon et al.[19]

The molecular weight and polydispersity (PDI) of the polymers were measured with size exclusion chromatography (SEC). The functionality of PS-$NH_2$ was determined by coupling it with an excess of PMMA-anh in dry THF. The reaction was brought to completion by heating the solution at 70 °C for at least 24 h, and the PS-$NH_2$ conversion was measured with a UV detector on the SEC described below. The amine functionality was also measured with a fluorine NMR method recently developed in our lab.[20] The two methods gave equivalent results, as shown in Table 1. The functionality of PMMA-anh-pyr was determined by coupling it with excess PS-$NH_2$ in dry THF solution at 70 °C for 24 h. The PMMA-anh-pyr conversion was measured with the fluorescence detector on SEC.

**Sample Preparation.** Bilayer samples were constructed by sequentially spin-coating polymer solutions onto a silicon substrate. For example, a PMMA-anh-pyr solution in toluene (ca. 4.0 wt %) was first spun onto a silicon wafer and dried overnight. A Tencor profilometer indicated that the film thickness was ~150 nm. The second layer was prepared by spin-coating a PS solution (ca. 4.0 wt %, could be a mixture of PS-$NH_2$/PS-CN) in a cyclohexane/toluene mixed solvent (87/13 v/v) onto the PMMA film. This particular mixed solvent does not dissolve or perturb the PMMA layer, as checked by AFM.[17] Samples for both reaction conversion and interfacial topography measurements were prepared in this way. They were annealed at 175 °C under vacuum for various reaction time intervals, followed by quenching in liquid nitrogen prior to analysis.

For TEM, the polymer solutions were spun onto two separate epoxy substrates, which were molded from a standard epoxy kit (Polybed 812, Polysciences Inc.). The two films were separately annealed for 10 min at 175 °C under vacuum and were then pressed together by hand between the two substrates. Then the whole sample was further annealed for 1 h at 175 °C before being quenched with nitrogen gas.

**Atomic Force Microscopy (AFM).** Before AFM analysis, each bilayer sample was immersed in an 87/13 v/v cyclohexane/toluene mixture solvent for 12 h to remove the top PS layer, followed by drying under vacuum for another 12 h. The revealed interface was examined using AFM with a Nanoscope III Multimode system (Digital Instruments) in tapping mode. All the data were acquired in height mode with scan rate of 1 Hz and scan size of 10 × 10 $\mu$m, corresponding to a probe movement of 20 $\mu$m/s. The root-mean-square (RMS) roughness was evaluated by analyzing the 2-dimensional (2D) height image with the Nanoscope software.

**Size Exclusion Chromatography (SEC)/Fluorescence Analysis.** The bilayer samples for SEC/fluorescence analysis were completely dissolved in about 1 mL of THF. Two drops of phenyl isocyanate were added to quench any unreacted amine groups. 100 $\mu$L of the solution was then injected into a Waters 590 SEC equipped with three Phenomenex Phenogel columns (5 $\mu$m bead size), an internal refractive index detector (Water 410), an external UV detector (Spectroflow 757, Kratos Analytical Instruments), and an external fluorescence detector (F-1050, Hitachi). For amine functionality determination, the UV detector was used to measure the reaction conversion with a wavelength of 254 nm for PS. For all the other reactions in this work, the fluorescence detector was used to measure the PMMA-anh-pyr conversions with excitation and emission wavelengths of 348 and 396 nm, respectively. The detailed procedures for extracting conversion from the SEC traces are described elsewhere.[19]

**Transmission Electron Microscopy (TEM).** The sandwiched samples prepared for TEM were microtomed to ca. 60 nm thick slices at room temperature with a diamond knife.

**Scheme 1. Synthesis of (a) Amine-Terminal PS and (b) Pyrene-Labeled PMMA-anh by ATRP**

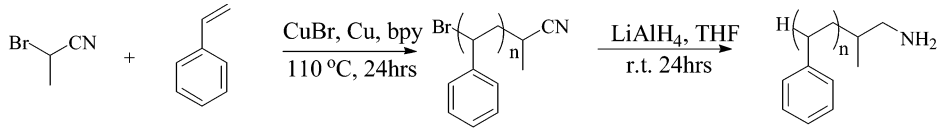


(a) PS-$NH_2$

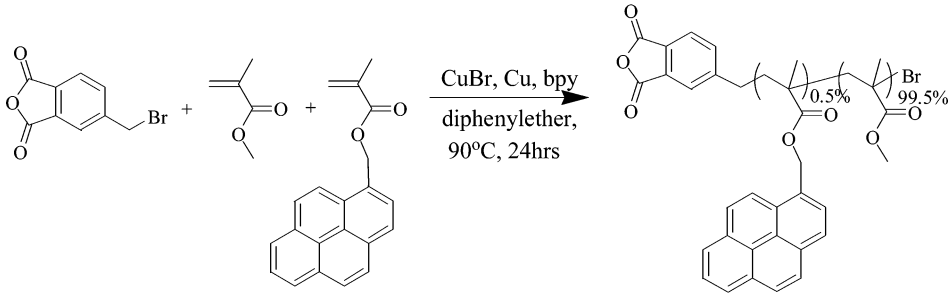


(b) PMMA-anh-pyr

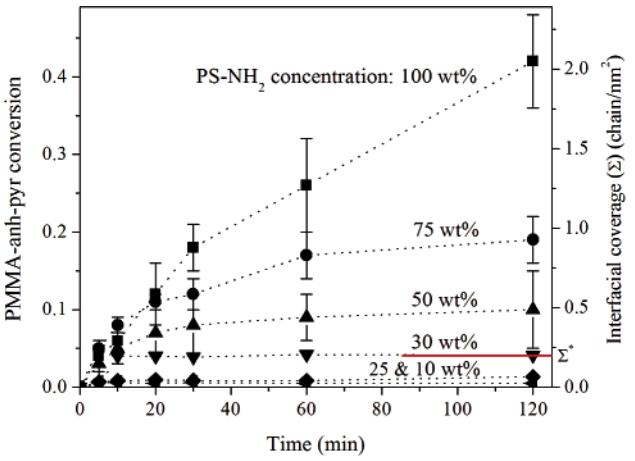


**Figure 1.** PMMA-anh-pyr conversion (left axis) and block copolymer interfacial coverage (Σ, right axis) vs annealing time for different PS-$NH_2$ concentrations: ■, 100 wt %; ●, 75 wt %; ▲, 50 wt %; ▼, 30 wt %; ◆, 25 wt %; tilted ▲, 10 wt %. All the samples were annealed at 175 °C, and Σ was calculated from PMMA-anh-pyr conversion.

The PS phase was selectively stained with $R_uO_4$ (0.5% aqueous solution) to increase the contrast. The morphology was observed with TEM on a JEOL 1210 at 120 keV.

## Results and Discussion

**Reactions at Short Time.** In this work we focus on the early time regime of the reaction.[6,11,21] The first reaction conversion was measured after putting the sample into a preheated oven for 5 min. One pertinent question is whether 5 min is long enough for the bilayer film to reach the set temperature. Considering heat transfer in the oven, the temperature profile of the silicon wafer can be estimated with an unsteady state heat conduction model.[22] Following this model, the time for the center of the silicon wafer to reach 175 ± 2 °C is less than 1 s. Since the thin polymer film is located at the surface of the wafer, it should take significantly less time to approach the set temperature, and therefore the heat transfer time is negligible.

As shown in Figure 1, significant conversion was detected for all the samples after 5 min annealing. For the samples with 50 wt % or higher PS-$NH_2$, about 4% PMMA-anh-pyr is consumed within 5 min. For the samples with 30 wt % or less PS-$NH_2$, the conversions are lower but still significant. Clearly even though the absolute conversion values depend on PS-$NH_2$ concentration, the initial coupling reaction at a PS/PMMA static interface is not as slow as had been suspected.[6,8,12] At longer annealing times, the reaction conversion increased substantially for 50% or greater reactive PS but hardly at all for the lower concentrations. This low conversion for low concentration of reactive groups is in agreement with previous work.[5,6]

To further confirm the reaction at short times, the interfacial morphology development was observed with AFM. As shown in the first two panels of Figure 2 for the 75 wt % PS-$NH_2$ case, the PMMA-anh-pyr surface topographies before and after annealing for 5 min are totally different. (Notice that both images have the same scale bar in the vertical direction.) Prior to annealing, the interface is flat and smooth. After annealing for 5 min, the interface becomes significantly rough. Since the interface between PS-CN/PMMA-anh-pyr (not shown) remains flat after 1 h annealing, this roughening is attributed to block copolymer formation at the interface.

**Interfacial Coverage Development.** The interfacial coverage (Σ) may be defined as the number of block copolymer chains formed per unit interfacial area. It can be calculated from the PMMA-anh-pyr conversion measured by SEC using eq 1, assuming a flat interface between PS and PMMA.

$$\Sigma = \frac{l\alpha\rho N_{AV}}{M_n} \tag{1}$$

Here $l$ is the thickness of the PMMA-anh-pyr layer, $\rho$, $\alpha$, and $M_n$ are the density, the conversion, and the number-average molecular weight of PMMA-anh-pyr, respectively, and $N_{AV}$ is Avogadro's number. The interfacial coverage development with annealing time is also summarized in Figure 1 (the right axis). Generally, as the annealing time increases, Σ increases, but Σ does not continuously increase until the limiting reagent PS-$NH_2$ is consumed. Beyond a certain time or Σ, the coupling reaction slows down or stops. Similar phenomena may be found in other reports.[6,11−13,21] The time to reach the leveled-off conversion is defined as $t_s$ here. As summarized in Table 2 for different PS-$NH_2$ concentrations, $t_s$ increases with PS-$NH_2$ concentration. For pure PS-$NH_2$, Σ continuously increases over the whole annealing time (2 h in this case), although the rate perhaps slows down at long times. This result is consistent with previous work on pure PS-$NH_2$/PMMA-anh systems.[11,13] Jones reported that the reaction took about 8 h at 175 °C before the PMMA-anh conversion leveled off, for a pure PS−$NH_2$/PMMA-anh pair with similar molecular weights as ours.[11] When the PS-$NH_2$ concentration decreases from 75 to 30 wt %, $t_s$ decreases from 60 to 10 min. For the systems with 25 wt % or less PS-$NH_2$, Σ does not change much after the first sampling time. Probably, $t_s$ for these dilute PS-$NH_2$ systems are even less than 5 min. Schulze et al. studied the time evolution of the block copolymer interfacial excess ($z^*/R_g$) (which is comparable to Σ) for the dilute dPS-$NH_2$/PMMA-anh system.[6] It was found that $z^*/R_g$ continuously increases until 70 h. However, it should be noted that the time scale in that study was much larger than ours, and the first sampling time was 4 h, longer than our last sampling time.

The PS-$NH_2$ concentration not only affects $t_s$, but it also affects the value of the plateau in Σ ($\Sigma_s$). As shown in Figure 1, $\Sigma_s$ increases with PS-$NH_2$ concentration. When the PS-$NH_2$ concentration decreases from 75 to 30 wt %, $\Sigma_s$ is reduced from 0.81 to about 0.19 chains/nm$^2$. When PS-$NH_2$ is diluted down to 25 wt %, $\Sigma_s$ decreases to about 0.03 chains/nm$^2$. After that, further diluting PS-$NH_2$ does not change $\Sigma_s$ significantly. Here, it should be noted that although these are dilute systems, the time for PS-$NH_2$ to reach the interface is much less than 2 h. Thus, diffusion of functional polymer chains is not the limiting step for the coupling of PS-$NH_2$/PMMA-anh at flat interfaces.[6]

**Interfacial Roughness Development.** The topography of the exposed PMMA surface after removing the PS layer was observed with AFM. Figure 2 shows a sequence of images of the typical interfacial roughness development with annealing time for 75 wt % PS-$NH_2$/PMMA-anh-pyr. As shown, before annealing the interface is flat and smooth. After 5 min, the interface becomes significantly rough. Further annealing makes the interface slightly rougher, but from 10 min to 2 h, there is no obvious change in roughening in the 3D

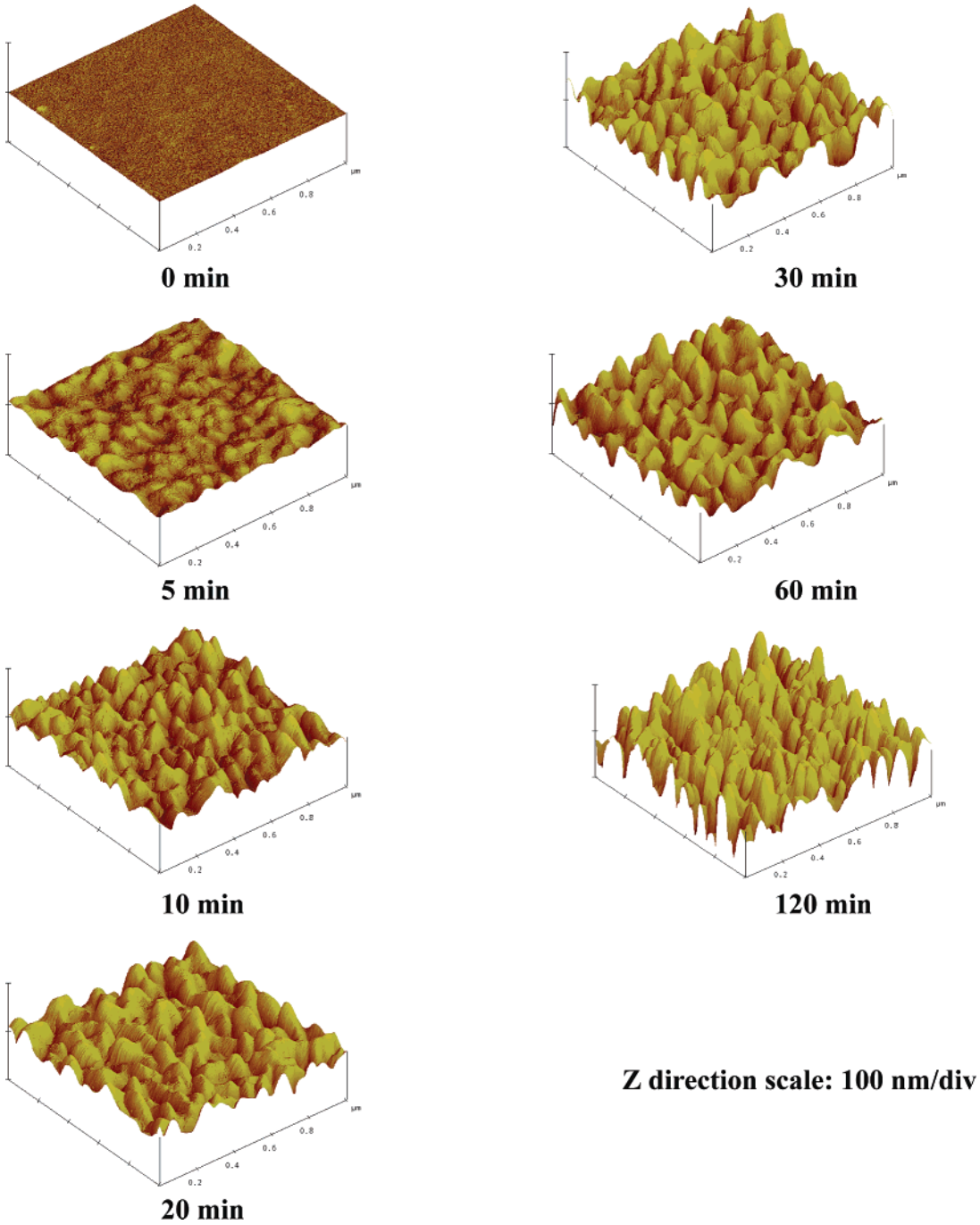


**Figure 2.** Interfacial roughness development at 175 °C for 75 wt % PS-$NH_2$/PMMA-anh-pyr measured with AFM.

**Table 2. Characteristics of the Coupling Reactions with Different PS-$NH_2$ Concentrations**

| PS-$NH_2$ (wt %) | Σ (chains/nm$^2$) 5 min | Σ (chains/nm$^2$) 10 min | $t_s$ (min) | $\Sigma_s$ (chains/nm$^2$) | Σ/Σ* at 60 min |
|---|---|---|---|---|---|
| 100 | 0.19 | 0.29 | | 1.67[a] | 6.2 |
| 75 | 0.18 | 0.26 | 60 | 0.81 | 4.1 |
| 50 | 0.18 | 0.23 | 30 | 0.33 | 2.2 |
| 30 | 0.02 | 0.19 | 10 | 0.19 | 1.0 |
| 25 | 0.03 | 0.03 | 5 | 0.03 | 0.2 |
| 10 | 0.03 | 0.03 | 5 | 0.03 | 0.2 |

[a] Interfacial coverage after 120 min. However, the coupling reaction was still continuing at 120 min. Jones et al. reported for 100% PS-$NH_2$ the reaction stops after about 8 h.[11]

images. To quantitatively analyze the interfacial roughening, the RMS roughness was extracted from the images shown in Figure 2 and is plotted vs time in Figure 3a. As shown, the RMS roughness increases to above 10 nm in about 10 min and then evolves to about 15 nm very slowly over 2 h. The RMS roughness development is consistent with the corresponding interfacial coverage development. As shown in Figure 1, the coupling reaction for this PS-$NH_2$ concentration also begins to slow down after 10 min. Figure 3a also shows the RMS roughness development for 10 wt % PS-$NH_2$. It increases to about 1.4 nm in the first 5 min and then remains about the same up to 2 h. Again, the interfacial roughness and reaction conversion developments are consistent. It should be noticed that the RMS roughness for the samples without annealing is not zero (around 0.5 nm). This is probably caused by surface thermal fluctuations and/or perturbation by the solvent treatment, but it is much less than that caused by the coupling reaction, even for dilute PS-$NH_2$.

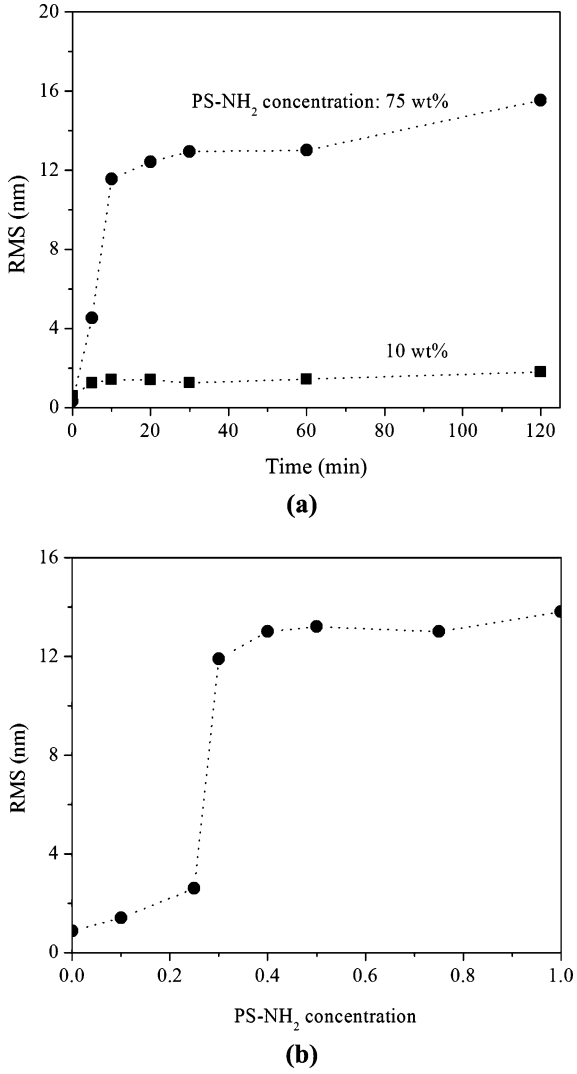


**Figure 3.** Root-mean-square (RMS) roughness vs (a) annealing time; (b) PS-$NH_2$ concentrations after 1 h annealing of PS-$NH_2$/PMMA-anh-pyr. All the samples were annealed at 175 °C.

Figure 3b plots the RMS roughness vs PS-$NH_2$ concentration for a constant annealing time of 1 h at 175 °C. As shown, the RMS roughness is modest for the samples with 25 wt % or less PS-$NH_2$. Upon increasing the PS-$NH_2$ concentration from 25 to 30 wt %, there is an abrupt increase in RMS roughness. After that, further increasing the PS-$NH_2$ concentration does not change the RMS roughness significantly. This result will be shown below to be due to the emulsification transition; however, AFM is not able to detect the emulsification directly. In other words, although the conversion increases at high concentrations, the RMS roughness remains nearly constant because a significant fraction of the emulsified material has been washed away.

To better understand the interfacial roughness development, the maximum interfacial coverage ($\Sigma^*$) at a PS/PMMA interface can be estimated by assuming a dense monolayer of block copolymer at the interface. The thickness of this hypothetical monolayer is half of the lamellar spacing in the corresponding ordered block copolymer phase. Thus, the maximum interfacial coverage can be estimated by eq 2.

$$\Sigma^* = \frac{\text{thickness of copolymer monolayer}}{\text{volume of one chain}} \qquad (2)$$

Using the empirical relationship between the interfacial area occupied by a block copolymer chain and the degree of polymerization of the copolymer developed by Russell et al. based on neutron reflectivity experiments,[23] $\Sigma^*$ is estimated to be ca. 0.2 chain/nm$^2$ for the PS-*b*-PMMA copolymer formed here. This may be compared to the interfacial coverage for the 25% and 30% PS-$NH_2$/PMMA-anh-pyr systems, where the sharp increase in interfacial roughness happens (Figure 3b). From Figure 1, we can see that $\Sigma^*$ falls just between $\Sigma$ for the 25% and 30% PS-$NH_2$ samples after 1 h of annealing. Thus, this sharp increase in roughness shown in Figure 3b is not an accident but may be attributed directly to the emulsification of the interface, which occurs when $\Sigma$ matches $\Sigma^*$. The interfacial roughness can therefore be separated into two regimes based on $\Sigma^*$. For $\Sigma < \Sigma^*$ the interfacial roughness increases with conversion but remains low. Once $\Sigma$ exceeds $\Sigma^*$, the interfacial roughness increases markedly but becomes an ill-defined quantity in the sense that there may no longer be a single interface in the system. The AFM measurements in this regime show a constant roughness, but this may be interpreted simply as a constant roughness of the surface that remains after washing off the top layer. In some of the measurements reported by Schulze et al.,[17] the apparent AFM roughness actually decreased with conversion at long times, presumably due also to the washing process after the formed copolymer had more opportunity to diffuse away, into the bulk of the layers.

As shown clearly in Figure 1, at high PS-$NH_2$ concentrations $\Sigma$ is much higher than $\Sigma^*$ during most of the annealing time. This phenomenon has been observed by many other researchers[11−13] and even for dilute functional polymer system after very long annealing times.[6] Physically, this is impossible at a flat interface. AFM shows that the interfaces become rough as the coupling reaction continues, and thus the total interfacial area between PS and PMMA increases accordingly. Using the Nanoscope software, the actual increase in interfacial area due to roughening may be estimated to be about 20% for an RMS roughness of 15 nm. Since interfacial coverage for pure PS-$NH_2$ after 1 h is about 6 times larger than $\Sigma^*$, roughening alone cannot explain this high value. This argument supports the interpretation given above that the sharp increase in roughening corresponds to the emulsification transition.

To obtain a more complete picture, TEM was used to observe the cross section of the interface. As shown in Figure 4, the interface between PS-CN/PMMA-anh-pyr is still flat after 1 h annealing, whereas for the 100 wt % PS-$NH_2$/PMMA-anh-pyr pair the interface becomes quite rough after the same time of annealing. Furthermore, a layer of emulsified material, about 100 nm thick, remains visible near the interface.

The roughness of the interface as observed via TEM and AFM may in fact be compared directly. As shown in Figure 5, the top image is a section of the interface from the TEM image in Figure 4b, but expanded in scale to match AFM. A jagged line, drawn by eye, suggests the main features of this interface. The lower image is a line section taken from the 2D AFM image of a sample annealed under the same conditions, i.e., 100% reactive PS concentration and 1 h reaction time. In this case the jagged line in the middle highlights the surface of the exposed PMMA layer. These two lines are remarkably similar, in both the fluctuation amplitude and the typical fluctuation wavelength. This observation con-

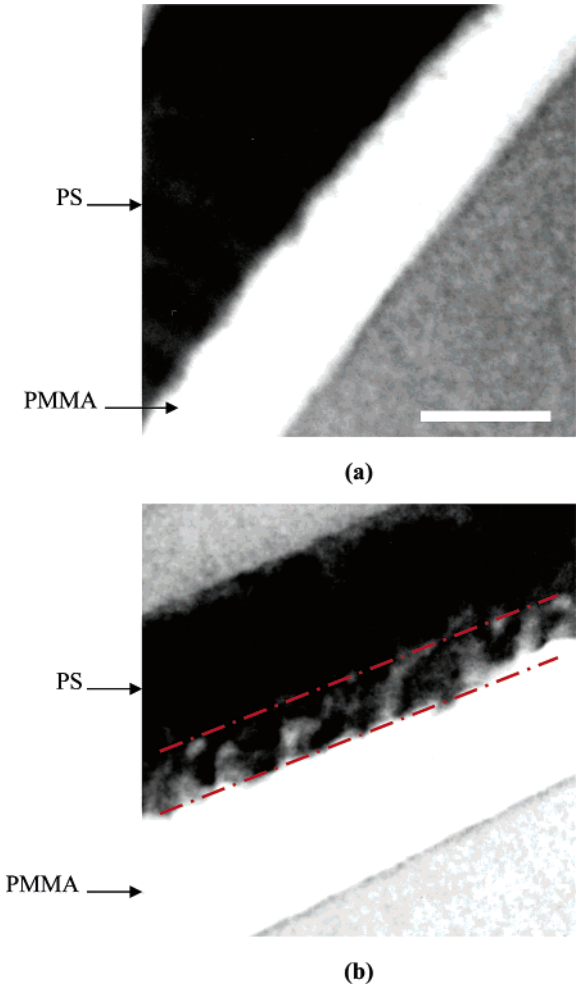


**Figure 4.** Interfacial roughening and emulsification observed with TEM. (a) PS-CN/PMMA-anh-pyr; (b) 100 wt % PS-$NH_2$/PMMA-anh-pyr. Both samples are annealed at 175 °C for 1 h. The scale bar is 200 nm.

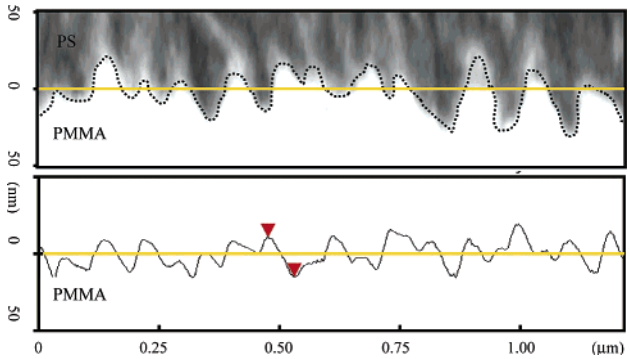


**Figure 5.** Interfacial roughness comparison between TEM (top) and AFM (bottom) for 100 wt % PS-$NH_2$/PMMA-anh-pyr. The interface from TEM image has been expanded to the same length scale as the AFM image. The AFM roughness is from a line roughness of the 2D scan.

firms that the entire emulsified region is removed by the selective solvent during the removal of the PS layer.

## Summary

The coupling reaction of PS-$NH_2$/PMMA-anh-pyr at a static interface is quite rapid in the initial stages. A certain amount of block copolymer is formed in a few minutes, and this leads immediately to a roughened interface. The block copolymer interfacial coverage and the extent of roughening depend strongly on the concentration of PS-$NH_2$. When the concentration is low, $\Sigma$ is lower than $\Sigma^*$ and does not change much with either annealing time or concentration. This results in a modest and almost concentration-independent interfacial roughness. When the concentration is increased to 30 wt %, $\Sigma$ exceeds $\Sigma^*$, and there is a large increase in RMS roughness. Further increasing PS-$NH_2$ concentration continues to increase $\Sigma$ (much higher than $\Sigma^*$) but has little further effect on RMS roughness. This is because AFM is always measuring an interface saturated with block copolymers when $\Sigma > \Sigma^*$; the excess material has been emulsified and is washed away in the AFM sample preparation step. Direct TEM cross-sectional imaging of the interface supports this picture.

**Acknowledgment.** This research has been supported in part by the MRSEC program of the National Science Foundation under Award DMR-0212302 and IPRIME (the Industrial Partnership for Research in Interfacial and Materials Engineering) at the University of Minnesota. J.Z. thanks Prof. Tom Hoye, Dr. Hyun K. Jeon, and Shengxiang Ji for helpful discussions about the synthesis and conversion extraction. J.Z. also appreciates the help of Kwanho Chang with TEM.

## References and Notes

(1) Baker, W.; Hu, G. *Reactive Polymer Blending*; Hanser Publisher: Munich, 2001.
(2) Koning, C.; Van Duin, M.; Pagnoulle, C.; Jerome, R. *Prog. Polym. Sci.* **1998**, *23*, 707.
(3) Paul, D. R.; Bucknall, C. B. *Polymer Blends*; Wiley: New York, 2000; Vol. 2.
(4) Lyu, S.-P.; Cernohous, J. J.; Bates, F. S.; Macosko, C. W. *Macromolecules* **1999**, *32*, 106.
(5) Jiao, J.; Kramer, E. J.; de Vos, S.; Moeller, M.; Koning, C. *Macromolecules* **1999**, *32*, 6261.
(6) Schulze, J. S.; Cernohous, J. J.; Hirao, A.; Lodge, T. P.; Macosko, C. W. *Macromolecules* **2000**, *33*, 1191.
(7) Oyama, H. T.; Inoue, T. *Macromolecules* **2001**, *34*, 3331.
(8) Kim, H. Y.; Jeong, U.; Kim, J. K. *Macromolecules* **2003**, *36*, 1594.
(9) O'Shaughnessy, B.; Sawhney, U. *Phys. Rev. Lett.* **1996**, *76*, 3444.
(10) O'Shaughnessy, B.; Sawhney, U. *Macromolecules* **1996**, *29*, 7230.
(11) Jones, T. D.; Schulze, J.; Macosko, C. W.; Moon, B.; Lodge, T. P. *Macromolecules* **2003**, *36*, 7212.
(12) Jeon, H. K.; Macosko, C. W.; Moon, B.; Hoye, T. R.; Yin, Z. *Macromolecules* **2004**, *37*, 2563.
(13) Yin, Z.; Koulic, C.; Pagnoulle, C.; Jerome, R. *Langmuir* **2003**, *19*, 453.
(14) Guegan, P.; Macosko, C. W.; Ishizone, T.; Hirao, A.; Nakahama, S. *Macromolecules* **1994**, *27*, 4993.
(15) Orr, C.; Cernohous, J.; Guegan, P.; Hirao, A.; Jeon, H.; Macosko, C. *Polymer* **2001**, *42*, 8171.
(16) Fredrickson, G. H. *Phys. Rev. Lett.* **1996**, *76*, 3440.
(17) Schulze, J. S. Ph.D. Thesis, University of Minnesota, 2001.
(18) Malz, H.; Komber, H.; Voigt, D.; Hopfe, I.; Pionteck, J. *Macromol. Chem. Phys.* **1999**, *200*, 642.
(19) Moon, B.; Hoye, T. R.; Macosko, C. W. *Polymer* **2002**, *43*, 5501.
(20) Ji, S.; Hoye, T. R.; Macosko, C. W. *Macromolecules* **2005**, *38*, 4679.
(21) Oyama, H. T.; Ougizawa, T.; Inoue, T.; Weber, M.; Tamaru, K. *Macromolecules* **2001**, *34*, 7017.
(22) Bird, R. B.; Stewart, W. E.; Lightfoot, E. N. *Transport Phenomena*; John Wiley & Sons: New York, 2002.
(23) Anastasiadis, S.; Russell, T.; Satija, S.; Majkrzak, C. *J. Chem. Phys.* **1990**, *92*, 5677.

MA050530L